Observation of bound and antibound states of cavity polariton pairs in a CuCl microcavity

S. Matsuura,[1] Y. Mitsumori,[1,*] H. Kosaka,[1] K. Edamatsu,[1] K. Miyazaki,[2] D. Kim,[2] M. Nakayama,[2] G. Oohata,[3] H. Oka,[4] H. Ajiki,[5] and H. Ishihara[6]

[1]*Laboratory for Nanoelectronics and Spintronics, Research Institute of Electrical Communication, Tohoku University, Sendai 980-8577, Japan*

[2]*Department of Applied Physics, Graduate School of Engineering, Osaka City University, Osaka 558-8585, Japan*

[3]*Department of Physical Science, Osaka Prefecture University, Osaka 599-8531, Japan*

[4]*Institute for Research Promotion, Niigata University, Niigata 950-2102, Japan*

[5]*Photon Pioneers Center, Osaka University, Osaka 565-0871, Japan*

[6]*Department of Physics and Electronics, Osaka Prefecture University, Osaka 599-8531, Japan*

(Received 7 January 2013; revised manuscript received 27 December 2013; published 31 January 2014)

We observed the antibound state, as well as the bound state, for cavity polariton pairs in a planar CuCl microcavity by spectrally resolved four-wave mixing. We obtained dispersion curves of the bound and antibound states by changing the incident angle of the pump pulses corresponding to the cavity detuning. The dispersion curve for the bound state suggests that the bound state is mainly composed of a bare biexciton and is weakly coupled to the cavity photons. The dephasing time of the bound state was faster than that of a bare biexciton in a thin sample, supporting the hypothesis that the bound state is coupled to the cavity photons. On the other hand, the antibound state consists of two lower polaritons having the same spin. The clear observation of the antibound state can be qualitatively explained by the phase-space filling, which reduces the Rabi splitting.

DOI: 10.1103/PhysRevB.89.035317 PACS number(s): 71.36.+c, 78.47.J−, 42.50.Md

An exciton in a planar semiconductor microcavity strongly interacts with a cavity photon confined between the distributed Bragg reflectors, forming a cavity polariton as a hybrid quantum state. This cavity polariton exhibits unique optical properties, such as Bose-Einstein condensation [1] and parametric amplification [2]. In the optical effects arising from the many-body effects of the cavity polaritons, the attractive and repulsive interactions among the polaritons play key roles. These interactions also occur between the two cavity polaritons, as the lowest order of the many-body effects. It is well known that the attractive interaction between two polaritons with opposite spins forms an energetically stable *bound state* (BS), i.e., biexcitons [3,4] or bipolaritons [5], with the total angular momentum $J = 0$. On the other hand, the *antibound state* (AS) for the polariton pairs with $J = 2$, which results from the repulsive interaction between the two polaritons with the same spins, is expected to show negative binding energy (antibinding energy) leading to an unstable state. Recently, the BS of cavity polariton pairs has begun to attract a great deal of attention because of theoretical proposals that it can be used for highly efficient entangled photon pair generation [6,7], a squeezed light source [8], and electromagnetically induced transparency (EIT) material [9]. In the experimental studies, there have been only a few reports on observations of the BS in microcavities based on III-V compound semiconductors [3–5,10] and II-VI compounds [11]. On the other hand, the AS has not yet been observed in the cavity polariton system, as can be seen in the bare exciton system in wide-gap II-VI based quantum wells [12,13]. Therefore, an experimental study on the optical properties of the BS and AS for cavity polariton pairs should provide basic knowledge of many-body effects in microcavities and contribute to the development of semiconductor-based quantum information-communication devices.

Based on the recent technique for growing planar semiconductor microcavities, various wide-gap semiconductor-based microcavities realizing a strong-coupling regime have been developed, such as materials based on CuCl [14–16], ZnO [16–19], and GaN [20–22], as well as ZnSe [23,24]. In such materials, giant vacuum Rabi splitting has been observed even in low-quality-factor (Q) cavities, owning to the large oscillator strength of the bare excitons [14–20,22]. Moreover, at room temperature, polariton lasing [25] can also be observed, as well as the vacuum Rabi splitting [16,17,21,22,24]. Hence, a wide-gap semiconductor-based microcavity system becomes one of the interesting physical systems showing new optical effects. In addition, the strong Coulomb interaction between the two bare excitons in wide-gap semiconductors gives large binding energy to the biexcitons, suggesting that these wide-gap semiconductor-based microcavities are suitable for the study of the BS and AS of cavity polariton pairs

In this paper, we report on the optical properties of the BS and the AS of cavity polariton pairs in a planar CuCl microcavity observed by the spectrally resolved four-wave mixing (FWM) technique within the third-order nonlinear optical process. We obtained the dispersion relations of the BS and AS by changing the incident angle of the pump pulses corresponding to cavity detuning. The dispersion curve of the BS suggests that the BS is composed of almost the bare biexciton and is weakly coupled to the cavity photons through the unbound two-polariton states. The dephasing time of the BS was faster than that of the bare biexciton in a thin sample, supporting the presence of weak coupling. The AS exhibited a similar dispersion curve to the lower polariton (LP), indicating that the AS consists of two LPs with the same spins. The phase-space filling, which reduces the Rabi splitting, can qualitatively explain our clear observation of the AS in the FWM spectra. Our experimental results can contribute to

*mitumori@riec.tohoku.ac.jp

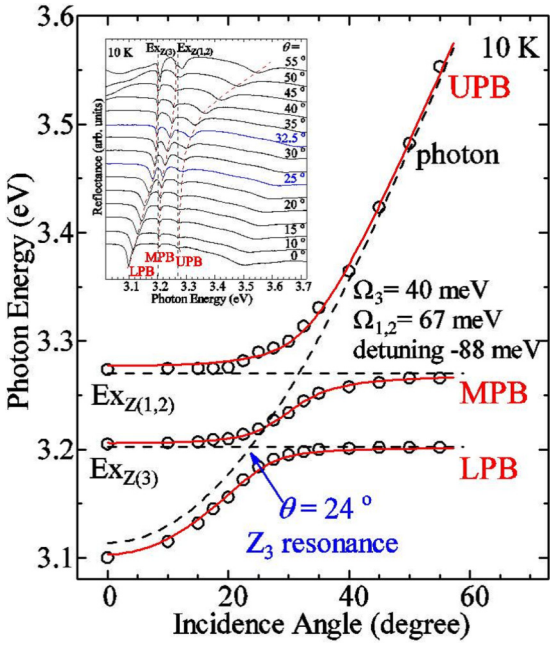

FIG. 1. (Color online) Dip positions in the reflection spectra of the CuCl microcavity as a function of the incident angle. Red lines are fitting curves using a 3×3 phenomenological Hamiltonian with parameters $\hbar g_3 = 20$ meV, $\hbar g_{1,2} = 33$ meV, $\Delta = -88$ meV. Dashed lines are the dispersion curves of the $Z_{1,2}$ and Z_3 excitons and the cavity photon mode. Inset: Angle-resolved reflection spectra of the CuCl microcavity obtained at 10 K. LPB, MPB, and UPB represent the lower, middle, and upper polariton branches, respectively.

the understanding of the many-body effects among the cavity polaritons.

The cavity structure in this work consists of a $\lambda/2$-long Fabry-Perot cavity sandwiched by distributed Bragg reflector mirrors consisting of 8 (10) pairs of HfO_2-SiO_2 layers for the top (bottom) mirror grown on a sapphire substrate. The quality factor of the cavity was $Q \sim 300$. A 50-nm-thick CuCl active layer was placed at the node of the electric field at the center of the cavity. For more details on the fabrication procedures of CuCl microcavities, see Refs. [14] and [15].

The inset in Fig. 1 shows the angle-resolved reflection spectra of the CuCl microcavity at 10 K. We can clearly observe three dips in the reflection spectra. These dip positions shift to the higher-energy side with increasing incident angle, indicating that three-level (lower, middle, and upper) cavity polaritons are formed in our microcavity. The three-level polaritons originate from the presence of the $Z_{1,2}$ and Z_3 excitons near the cavity resonance. We plot the energy positions of these polaritons as functions of the incident angle θ in Fig. 1. To estimate the exciton-cavity coupling $\hbar g_3$ ($\hbar g_{1,2}$) for the Z_3 ($Z_{1,2}$) exciton, we calculated the dispersion relations of these polariton branches using the phenomenological 3×3 Hamiltonian introduced in Ref. [14] and fitted them to the observed dip positions, as shown by the red curves in Fig. 1. We obtained $\hbar g_3 = 20$ meV, $\hbar g_{1,2} = 33$ meV, and the cavity detuning $\Delta = E_{Z_3} - E_C = -88$ meV, where E_{Z_3} and E_C are the Z_3 exciton energy and the photon energy at the cavity resonance for $\theta = 0°$, respectively. The large negative cavity detuning of the sample at the normal incidence

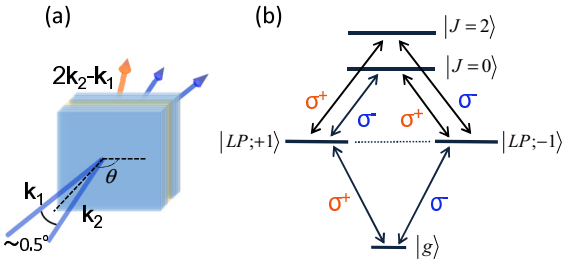

FIG. 2. (Color online) (a) Schematic view of the FWM experiment. (b) The polarization selection rule of a five-level system. $|g\rangle$ represents the ground state. $|J=0\rangle$ and $|J=2\rangle$ are the bound and antibound states for the polariton pairs, respectively. $|LP;\pm1\rangle$ are the lower polariton states having orbital angular momentums of ±1.

allowed us to investigate the positive and negative cavity detuning effects of the BS and the AS for the polariton pairs by changing the incident angle of the pump pulses around $\theta \sim 28°$, where the cavity detuning is $\Delta \sim 0$ meV. Note that the Z_3 ($Z_{1,2}$) exciton corresponds to the split-off-hole exciton (the degenerate heavy-hole and light-hole excitons) and that the Z_3 exciton is the lowest-energy excitonic state in the CuCl crystal [26].

The spectrally resolved FWM experiment was performed under transmission geometry using the second harmonic light of a femtosecond mode-locked Ti:sapphire laser. The central photon energy of the pump light was tuned to 3.186 eV, which corresponds to the two-photon resonant energy of the biexciton in CuCl bulk crystal. The bandwidth of the pump pulse was set to 25 meV and the temporal duration of the pulse was ~100 fs. The pump pulse was divided into two pulses with a time delay τ and focused again on the same spot on the sample. The angle between the first pulse with wave vector $\mathbf{k}_1$ and the second pulse with $\mathbf{k}_2$ was set to be as small as 0.5°. The FWM signal along $2\mathbf{k}_2$-$\mathbf{k}_1$ passing through the sample was fed into a spectrometer followed by a photomultiplier to observe the FWM spectra. We measured the FWM spectra by varying the time delay τ between the two pump pulses and the incident angle θ, i.e., the mean incident angle of the two pump pulses to the sample, as shown in Fig. 2(a). The samples for the FWM experiment were kept in a cryostat at 3.3 K.

Figure 3 shows the FWM spectra for $\tau = -200, 0$, and 200 fs at $\theta = 31°$. The pump pulses were in cocircular polarizations in Fig. 3(a), in cross-linear polarizations in Fig. 3(b), and in parallel-linear polarizations in Fig. 3(c). In these measurements, the excitation densities of the two pump pulses were set to be $I_1 = I_2 \sim 0.1$ μJ/cm^2 per pulse. Figure 3(d) shows the excitation density dependence of the FWM signal intensity at $\tau = 0$ fs under cocircular excitation. The signal intensity shows the third-order power dependence, indicating that our measurements were performed within the third-order nonlinear optical process and that it is reasonable to discuss the experimental results in the framework of the third-order optical nonlinearity.

The FWM spectra of the cocircular polarization excitation in Fig. 3(a) show single peaks at all the time delays, and those energy positions are different from each other. We infer that the peak at 3.194 eV at $\tau = 200$ fs is attributable to the transition between the LP and the ground state (GS), because the peak

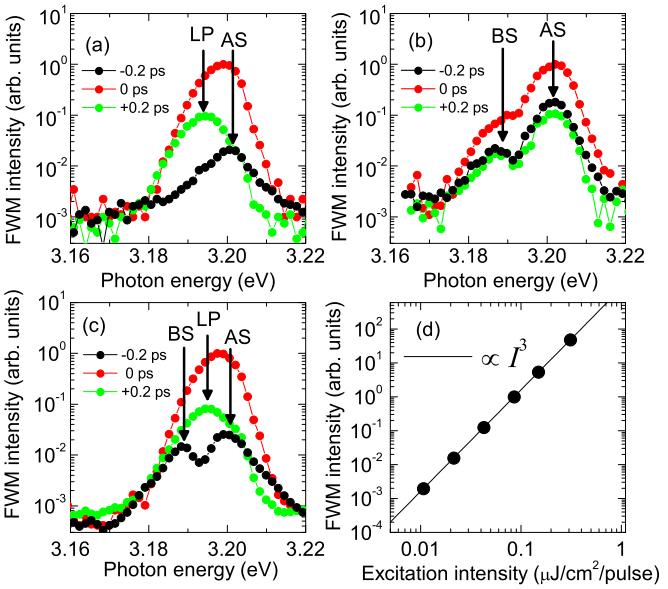

FIG. 3. (Color online) FWM spectra observed at $\tau = -200$, 0, and +200 fs for the (a) cocircular pump, (b) cross-linear pump, and (c) parallel-linear pump polarizations. (d) The excitation density (I) dependence of the peak intensity of the FWM spectrum at $\tau = 0$ fs under the cocircular pump polarization. The excitation densities of the first and second pulses were the same: $I = I_1 = I_2$.

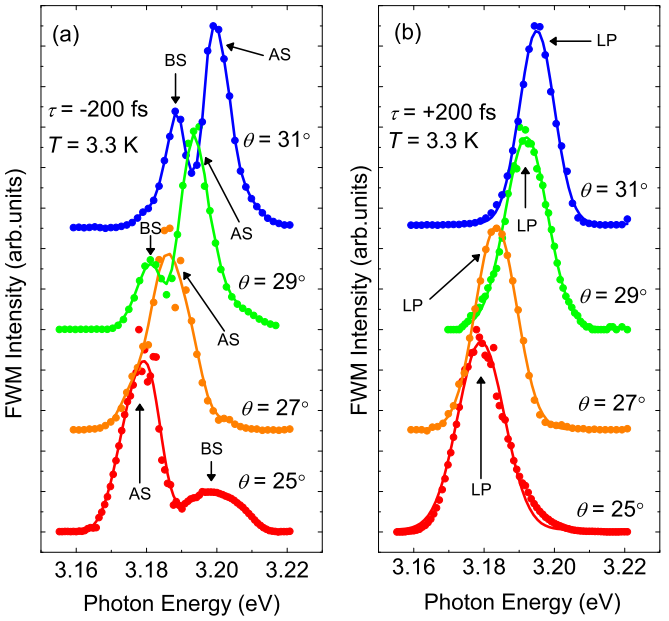

FIG. 4. (Color online) Incident-angle dependence of the FWM spectrum at (a) $\tau = -200$ fs and (b) $\tau = 200$ fs under the parallel-linear pump polarization.

position agrees with the dip in the linear reflection spectrum in Fig. 1. At $\tau = -200$ fs, the peak position locates at 3.202 eV, which is the higher-energy side compared with that of the LP. In the third-order nonlinear optical process for the FWM at the negative time delay in a simplified five-level system involving the $J = 0$ BS and the $J = 2$ AS illustrated in Fig. 2(b), the circularly polarized second pulse with wave vector $\mathbf{k}_2$ at $\tau < 0$ creates the $J = 2$ AS with the mode $2\mathbf{k}_2$ and then, at $\tau = 0$, the excitation of the $J = 2$ AS by the first pulse with $\mathbf{k}_1$ generates FWM signals along $2\mathbf{k}_2$-$\mathbf{k}_1$, which are emitted by the nonlinear polarization of the AS-LP and LP-GS transitions. Because the signal peak position at $\tau < 0$ differs from that of the LP, as seen in Fig. 3(a), we infer that the FWM signal at $\tau < 0$ in our result is mainly attributed to the AS-LP transition.

As shown in Fig. 3(b), the FWM spectrum at $\tau = 200$ fs in the cross-linear excitation exhibits a large peak at 3.202 eV and a small peak at 3.188 eV. The energy position of the large peak coincides with the value of the peak position observed in the cocircular excitation at $\tau = -200$ fs. It is generally known in the FWM experiment in an exciton system that the cross-linear polarization configuration at a positive time delay suppresses the signal of the transition from the single exciton state to the GS. The transitions from the exciton-pair states with $J = 0,2$ to the single exciton state contribute to the FWM signal [12]. Therefore, this agreement with the peak positions observed in the cocircular excitation at $\tau = -200$ fs and the cross-linear polarization at $\tau = 200$ fs supports our assignment of the AS observed in the cocircular excitation at $\tau = -200$ fs. The small peak observed at 3.188 eV in Fig. 3(b) originates from the $J = 0$ BS, which needs both left (σ^+) and right (σ^-) circular polarization components in the pump pulses for the creation. At $\tau = -200$ fs, we observed two peaks originating from the BS and the AS, the same as in the case at the positive time delay $\tau = 200$ fs.

From the above analysis, we can assign each peak in the FMM spectra in the parallel-linear polarization excitation, as shown in Fig. 3(c). The large peak at 3.202 eV and the small peak at 3.188 eV at $\tau = -200$ fs correspond to the AS-LP and BS-LP transitions, respectively. The single peak at $\tau = 200$ fs originates from the LP-GS transition. There have been reports on the observation of BS-LP transitions in parallel-linear polarization even at positive time delays [4]. In our experiment, the broad linewidth of the LP and the shift of the main peak between the negative and positive time delays disturbed the observation of the BS at positive time delays.

Figure 4 shows the FWM spectra in the parallel-linear polarization excitation for various pump incident angles θ at $\tau = -200$ fs for (a) and $\tau = 200$ fs for (b). As θ decreased, the spectral position of the LP peak in the FWM spectrum observed at $\tau = 200$ fs shifted to the lower-energy side, in accordance with the dispersion relation of the LP shown in Fig. 1. The energy position of the AS showed almost the same dependence of the LP on θ. On the other hand, the peak originating from the BS was overlapped by the AS peak at $\theta = 27^\circ$ and then was restored on the higher-energy side of the AS peak. In Fig. 5(a), we plot as functions of θ the peak positions of the LP observed at $\tau = 200$ fs and the BS and the AS at $\tau = -200$ fs in the FWM spectra at parallel-linear polarization excitation. We added the dispersion curve (dashed curve) of the LP branch obtained from Fig. 1 and the energy difference (solid curve) $E_{\mathrm{BX}\rightarrow\mathrm{LP}} = E_{\mathrm{BX}} - E_{\mathrm{LP}}$ between the bare biexciton energy $E_{\mathrm{BX}} = 6.372$ eV in a CuCl bulk crystal and the LP energy E_{LP}.

We observed that the positions of the LP peak followed the dispersion curve for the LP obtained by the linear reflection spectra, suggesting that our excitation density stayed

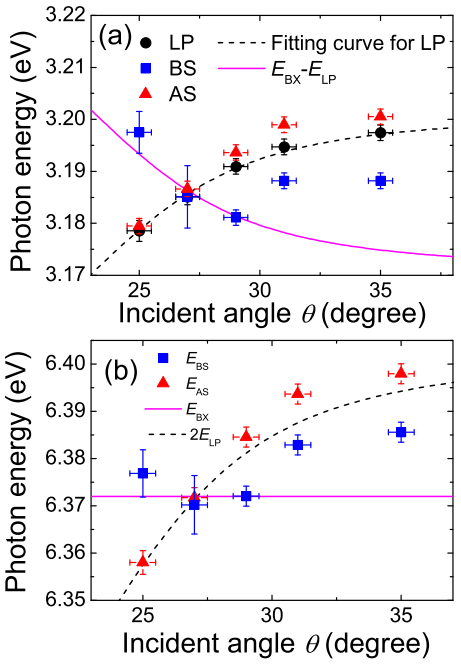

FIG. 5. (Color online) (a) Peak positions of the lower polariton, bound, and antibound states observed in the FWM spectra plotted as functions of the incident angle of the pump. Also plotted are the fitting curve for the dispersion curve of the lower polariton obtained from Fig. 1 and the energy difference, $E_{BX\rightarrow LP} = E_{BX} - E_{LP}$, between the biexciton in a bulk crystal, E_{BX}, and the lower polariton, E_{LP}. (b) Dependences of the bound-state energy, E_{BS}, and the antibound-state energy, E_{AS}, on the incident angle, together with E_{BX} and $2E_{LP}$.

in the weak excitation regime because the high excitation density usually makes the exciton-photon coupling weaker and reduces the vacuum Rabi splitting [27]. The positions of the BS peak, which correspond to the transition energy $E_{BS\rightarrow LP}$ from the BS to the LP, almost followed the energy difference $E_{BX\rightarrow LP}$ at small incident angles, indicating that the BS is mainly composed of a bare biexciton. On the other hand, the dispersion curve of the signal peak position of the AS, which has the transition energy $E_{AS\rightarrow LP}$ from the AS to the LP, is similar to that of the LP. From this finding, we can conclude that the AS consists of two LPs with the same spins. In order to examine the relation of the energy position of each state to the incident angle, we plotted the BS energy $E_{BS} = E_{BS\rightarrow LP} + E_{LP}$ and the AS energy $E_{AS} = E_{AS\rightarrow LP} + E_{LP}$ as functions of θ in Fig. 5(b), together with the bare biexciton energy E_{BX} and twice the value of the fitting curve for the LP $2E_{LP}$ in Fig. 1. In the estimation of the values E_{BS} and E_{AS}, we used the peak energy of the LP in the FWM spectrum at each incident angle. For the small θ, E_{BS} and E_{AS} agree with E_{BX} and $2E_{LP}$ within the error bars, respectively. In the large-θ regime, the BS energy increased with θ and the AS energy shifted to the higher-energy side of $2E_{LP}$.

The energy shift of the BS in the large-θ regime suggests that the BS is not just a bare biexciton but is weakly coupled to the cavity photons. Recent theories regarding the BS in microcavities have predicted that weak coupling of the BS to the cavity photons is realized through the unbound two-polariton states [7,28]. Therefore, the wave function of the BS contains the component of the unbound two-polariton states, as well as the bare biexciton [7,28]. As a result, the fact that the lowest unbound two-polariton state energy $2E_{LP}$ is much larger than E_{BX} in the large-θ regime shifts the BS to the higher-energy side of the bare biexciton. However, this qualitative analysis should be carefully revisited by quantitative theoretical calculations because positive detuning increases the biexciton composition in the wave function of the BS [28], which makes the BS energy close to the bare biexciton energy. Nevertheless, our observation of the incident-angle dependence of the BS energy indicates a cavity-detuning effect for the BS, which results from the coupling of the BS to the cavity photons.

For the AS, previous studies in exciton systems in quantum wells have pointed out the importance of the lateral confinement [12,13], as in the case of quantum dots [29]. In our cavity, the CuCl active layer was uniformly grown, and the thickness of 50 nm was sufficiently larger than the exciton Bohr radius, such that the lateral confinement induced by the roughness of the sample surface would have been negligible. As a possible origin, we suspect the phase-space filling, which plays an important role in analyses of transient experiments on exciton systems [30] and microcavities [31,32]. Phase-space filling is known to arise from the Pauli exclusion principle of the electrons and holes whereby two identical fermions cannot occupy the same state simultaneously, thereby reducing the transition dipole moment between the $J = 2$ exciton pair state and the $J = 1$ single exciton state [30,31], compared with the transition between the single state and the GS. In the cavity system, positive detuning increases the composition of the excitons in the wave function of the LP, which makes it more difficult to excite the LP pairs with the same spin at positive detuning than at negative detuning. Therefore, the positive detuning gives a much greater reduction in the transition dipole moment between the AS and the single LP state. As a result, the exciton-photon coupling energy (Rabi splitting) for the pair state with the same spin is decreased by the positive detuning. This reduction of the Rabi splitting in the positive detuning regime gives a clear observation of the AS at the higher-energy side of $2E_{LP}$ at large θ. In addition, the large oscillator strength of the excitons in the CuCl crystal yielding the giant vacuum Rabi splitting of the microcavity contributes to our clear observation of the AS for polariton pairs as a sufficiently large peak shift from the LP peak in the FWM spectrum.

As shown in Fig. 4, the linewidths of the BS and the AS exhibit dependences on θ, similar to the dependence of the LP linewidth. We confirmed that each linewidth was insensitive to the pump power in our excitation power range, indicating that the changes in these linewidths are not due to power broadening, such as an excitation-induced dephasing effect. Generally, the increase by negative detuning of photon components having short lifetimes gives a fast dephasing time, causing a line broadening to the LP [33]. Our result indicating the dependence of the linewidth of the LP on θ is in agreement with this tendency. The change in the linewidth of the AS by θ originates from the same source as that of the LP because the AS is composed of two LPs. As for the BS, E_{BS} at a small incident angle locates at a higher energy than the lowest unbound two-polariton state with the energy $2E_{LP}$, suggesting

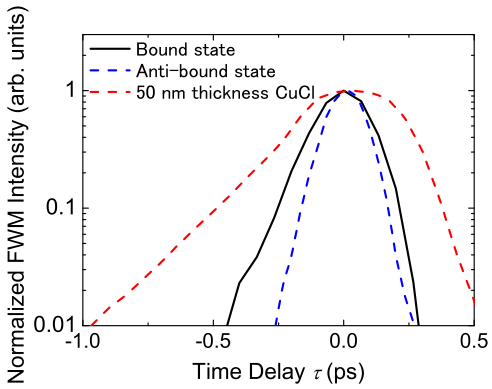

FIG. 6. (Color online) FWM responses monitored at the signal peak positions of the bound state and antibound state in the microcavity for $\theta = 31^\circ$, together with the biexciton in the 50-nm-thick CuCl film.

that the BS is no longer an energetically stable state. Therefore, the BS rapidly dissociates into two unbound polaritons. This enhancement in the dissociation gives the line broadening of the BS at small incident angles.

Next, we present the coherent dynamics of the BS in the microcavity. The solid curve in Fig. 6 represents the dependence on τ of the FWM signal intensity at the peak energy (3.188 eV) of the BS in Fig. 3(c) for $\theta = 31^\circ$. To compare the dephasing time with that of the bare biexciton, we performed an experiment on a CuCl thin-film sample having the same thickness (50 nm) as that of the active layer in our microcavity. The dashed red curve in Fig. 6 represents the results for the thin film monitored at the two-photon resonant energy of the biexciton. The decay time of the signal in the negative τ gives the two-photon coherence time of the BS and the bare biexciton [4,34]. Assuming that both samples are homogeneous systems, we estimated from Fig. 6 that the coherence time of the BS in the microcavity and that of the biexciton in the thin film were $\tau_{BS} = 170$ fs and $\tau_{BX} = 320$ fs, respectively. Neither coherence time depended on the excitation intensity in the range of our excitation densities, suggesting that Coulomb scatterings can be ruled out from the dephasing processes. It should be noted that our observed biexciton dephasing in the thin sample is much faster than the value ($T_2 \sim 20$ ps) reported for a much thicker sample, with a thickness of ~ 20 μm [35]. This difference of the observed dephasing time is attributable to the sample thickness. In practice, we have found that the biexciton dephasing time in thin films with a thickness from 50 to 200 nm is linearly proportional to the thickness, indicating that the main source of the dephasing process in the thin films is the propagation of the biexciton to the sample surface. Nevertheless, the dephasing time of the BS in the microcavity was considerably faster than that of bare biexcitons in the film samples. This experimental fact, even though indirectly, suggests the presence of cavity enhancement in the radiative rate (the Purcell effect) for the BS originating from the weak coupling to the cavity photons, which is similar to an exciton system in resonance with a low-Q cavity [36]. In our cavity, the exciton-photon coupling energy for the Z_3 exciton is $\hbar g_3 = 20$ meV, which is close to the bare biexciton binding energy $\Delta E_{BX} = 32$ meV. This condition is almost satisfied with the cavity resonance condition for the biexciton in a cavity, as predicted by recent theories [6,7]. Therefore, we infer that the cavity resonance effect shortens the radiative lifetime of the BS [6,7], which gives the BS in the cavity a faster dephasing time than the bare biexciton. Detailed experiments on the dephasing and energy relaxation processes of the BS are in progress.

Finally, we briefly mention the coherent dynamics of the AS and the dephasing time of the LP. As shown by the dashed blue curve in Fig. 6, both the signals for the AS in negative τ and the LP in the positive τ exhibit an instantaneous response for the pump pulse, suggesting that the two-photon coherence time of the AS and the dephasing time of the LP are comparable to the temporal duration of the excitation pulse, which results from the short lifetime of the cavity photons.

In conclusion, we observed an FWM signal originating from the $J = 0$ BS and $J = 2$ AS for cavity polariton pairs in a CuCl microcavity. The dispersion curves obtained by changing the incident angle of the pump pulses indicated that the BS was mainly composed of a bare biexciton and the AS consisted of two LPs with the same spins. The BS energy was almost the same as the bare biexciton energy at small incident angles but increased in large-incident-angle regimes. The dephasing time of the BS was faster than that of the bare biexciton in the thin sample. These experimental results indicated that the BS was weakly coupled to the cavity photons. The AS energy became larger than twice the value of the LP energy as the positive detuning increased; this result could be explained by phase-space filling. Our experimental findings should stimulate further studies of the optical properties of BS and AS of cavity polariton pairs in microcavities and contribute to the understanding of the many-body effects of cavity polaritons and the development of semiconductor-based quantum information-communication devices.

This work was supported by a Grant-in-Aid for Creative Scientific Research (Grant No. 17GS1204), a Grant-in-Aid for Scientific Research (Grant No. 22244035), and a Grant-in-Aid for Exploratory Research (Grant No. 24654081) from Japan's Society for the Promotion of Science.

[1] J. Kasprzak, M. Richard, S. Kundermann, A. Baas, P. Jeambrun, J. M. J. Keeling, F. M. Marchetti, M. H. Szymaska, R. André, J. L. Staehli, V. Savona, P. B. Littlewood, B. Deveaud, and L. S. Dang, Nature (London) **443**, 409 (2006).

[2] P. G. Savvidis, J. J. Baumberg, R. M. Stevenson, M. S. Skolnick, D. M. Whittaker, and J. S. Roberts, Phys. Rev. Lett. **84**, 1547 (2000).

[3] P. Borri, W. Langbein, U. Woggon, J. R. Jensen, and J. M. Hvam, Phys. Rev. B **62**, R7763 (2000).

[4] P. Borri, W. Langbein, U. Woggon, A. Esser, J. R. Jensen, and J. M. Hvam, Semicond. Sci. Technol. **18**, S351 (2003).
[5] T. Baars, G. Dasbach, M. Bayer, and A. Forchel, Phys. Rev. B **63**, 165311 (2001).
[6] H. Ajiki and H. Ishihara, J. Phys. Soc. Jpn. **76**, 053401 (2007).
[7] H. Oka and H. Ishihara, Phys. Rev. Lett. **100**, 170505 (2008).
[8] H. Oka and H. Ajiki, Phys. Rev. B **83**, 045305 (2011).
[9] F. Bassani, G. C. La Roccaa, and M. Artonib, J. Lumin. **110**, 174 (2004).
[10] X. Fan, H. Wang, H. Q. Hou, and B. E. Hammons, Phys. Rev. B **57**, R9451 (1998).
[11] U. Neukirch, S. R. Bolton, N. A. Fromer, L. J. Sham, and D. S. Chemla, Phys. Rev. Lett. **84**, 2215 (2000).
[12] T. Häupl, H. Nickolaus, F. Henneberger, and A. Schülzgen, Phys. Status Solidi B **194**, 219 (1996); H. Nickolaus and F. Henneberger, Phys. Rev. B **57**, 8774 (1998).
[13] H. Zhou, A. V. Nurmikko, C.-C. Chu, J. Han, R. L. Gunshor, T. Takagahara, Phys. Rev. B **58**, R10131 (1998).
[14] G. Oohata, T. Nishioka, D. Kim, H. Ishihara, and M. Nakayama, Phys. Rev. B **78**, 233304 (2008).
[15] M. Nakayama, K. Miyazaki, T. Kawase, and D. Kim, Phys. Rev. B **83**, 075318 (2011).
[16] T. Kawase, K. Miyazaki, D. Kim, and M. Nakayama, J. Appl. Phys. **112**, 093512 (2012).
[17] R. Shimada, J. Xie, V. Avrutin, Ü. Özgür, and H. Morkoč, Appl. Phys. Lett. **92**, 011127 (2008).
[18] M. Nakayama, S. Komura, T. Kawase, and D. Kim, J. Phys. Soc. Jpn. **77**, 093705 (2008).
[19] F. Médard, J. Zuniga-Perez, P. Disseix, M. Mihailovic, J. Leymarie, A. Vasson, F. Semond, and E. Frayssinet, Phys. Rev. B **79**, 125302 (2009).
[20] N. Antoine-Vincent, F. Natali, D. Byrne, A. Vasson, P. Disseix, J. Leymarie, M. Leroux, F. Semond, and J. Massies, Phys. Rev. B **68**, 153313 (2003).
[21] R. Butté, G. Christmann, E. Feltin, J.-F. Carlin, M. Mosca, M. Ilegems, and N. Grandjean, Phys. Rev. B **73**, 033315 (2006).
[22] I. R. Sellers, F. Semond, M. Leroux, J. Massies, M. Zamfirescu, F. Stokker-Cheregi, M. Gurioli, A. Vinattieri, M. Colocci, A. Tahraoui, and A. A. Khalifa, Phys. Rev. B **74**, 193308 (2006).
[23] P. Kelkar, V. Kozlov, H. Jeon, A. V. Nurmikko, C.-C. Chu, D. C. Grillo, J. Han, C. G. Hua, and R. L. Gunshor, Phys. Rev. B **52**, R5491 (1995).
[24] A. Pawlis, A. Khartchenko, O. Husberg, D. J. As, K. Lischka, and D. Schikora, Solid State Commun. **123**, 235 (2002).
[25] S. Christopoulos, G. Baldassarri Höger von Högersthal, A. J. D. Grundy, P. G. Lagoudakis, A. V. Kavokin, J. J. Baumberg, G. Christmann, R. Butté, E. Feltin, J. F. Carlin, and N. Grandjean, Phys. Rev. Lett. **98**, 126405 (2007).
[26] A. Goldmann, Phys. Status Solidi B **81**, 9 (1977); H. Overhof, *ibid.* **97**, 267 (1980).
[27] S. Jiang, S. Machida, Y. Takiguchi, and Y. Yamamoto, Appl. Phys. Lett. **73**, 3031 (1998).
[28] H. Oka and H. Ishihara, Phys. Rev. B **78**, 195314 (2008).
[29] S. V. Nair and T. Takagahara, Phys. Rev. B **55**, 5153 (1997).
[30] T. Aoki, G. Mohs, M. Kuwata-Gonokami, and A. A. Yamaguchi, Phys. Rev. Lett. **82**, 3108 (1999).
[31] M. Kuwata-Gonokami, S. Inouye, H. Suzuura, M. Shirane, R. Shimano, T. Someya, and H. Sakaki, Phys. Rev. Lett. **79**, 1341 (1997).
[32] Y. P. Svirko, M. Shirane, H. Suzuura, and M. Kuwata-Gonokami, J. Phys. Soc. Jpn. **68**, 674 (1999).
[33] X. Marie, P. Renucci, S. Dubourg, T. Amand, P. Le Jeune, J. Barrau, J. Bloch, and R. Planel, Phys. Rev. B **59**, R2494 (1999).
[34] W. Langbein and J. M. Hvam, Phys. Rev. B **61**, 1692 (2000).
[35] E. Vanagas, J. Kudrna, D. Brinkmann, P. Gilliot, and B. Hönerlage, Phys. Rev. B **63**, 153201 (2001).
[36] K. Tanaka, T. Nakamura, W. Takamatsu, M. Yamanishi, Y. Lee, and T. Ishihara, Phys. Rev. Lett. **74**, 3380 (1995).